Mon. Not. R. Astron. Soc. **290,** 119–138 (1997)

The Edinburgh–Durham Southern Galaxy Catalogue – VIII. The cluster galaxy luminosity function

S. L. Lumsden,[1★] C. A. Collins,[2★] R. C. Nichol,[3★] V. R. Eke[1★] and L. Guzzo[4★]

[1]*Anglo-Australian Observatory, PO Box 296, Epping, NSW 2121, Australia*
[2]*Astrophysics Group, School of Electrical Engineering, Electronics and Physics, Liverpool John Moores University, Byrom Street, Liverpool L3 3AF*
[3]*Department of Physics, Carnegie Mellon University, 5000 Forbes Avenue, Pittsburgh, PA 15213-3890, USA*
[4]*Osservatorio Astronomico di Brera, Via Bianchi 46, I-22055 Merate, Italy*

Accepted 1997 May 7. Received 1997 February 27; in original form 1996 July 23

ABSTRACT

We have re-examined the nature of the cluster galaxy luminosity function using the data from the Edinburgh–Durham Southern Galaxy Catalogue and the Edinburgh–Milano Redshift Survey. We derive a best-fitting luminosity function (LF) over the range -18 to -21 in $M(b_j)$, for a composite sample of 22 of the richer clusters that has $M(b_j)^* = -20.16 \pm 0.02$ and $\alpha = -1.22 \pm 0.04$. The dominant error in these values results from the choice of background subtraction method. From extensive simulations we can show that when the LF is fitted over this narrow range, it is difficult to discriminate against bright values of M^* in the single cluster fits, but that faint values provide a strong test of the universality of the luminosity function. We find that all the individual cluster data are well-fitted by a Schechter function with α fixed at -1.25, and that ≤ 10 per cent of these have fitted values of M^* that disagree from the average at the 99 per cent confidence level. We further show that fitting only a single parameter Schechter function to composite subsets of the data can give erroneous results for the derived M^*, as might be expected from the known tight correlation between M^* and α. By considering two parameter fits, the results of Monte Carlo simulations and direct two-sample χ^2 tests, we conclude that there is only weak evidence for differences between the data when broken down into subsets based on physical properties (Bautz–Morgan class, richness, velocity dispersion): from our simulations, only the evidence for a difference between subsets based on velocity dispersion may in fact be significant. However, we find no evidence at all that a Schechter function is not a good model for the intrinsic cluster luminosity function over this absolute magnitude range. Models that invoke strong evolution of galaxy luminosity of *all* galaxies within clusters are inconsistent with our results.

Key words: catalogues – galaxies: clusters: general – galaxies: luminosity function, mass function.

1 INTRODUCTION

The properties of the cluster galaxy luminosity function (LF) are still a matter of active debate. On the one hand, considerable stess has been laid on a single analytic expression for the LF, as determined by Schechter (1976), which it is argued holds true for all clusters and the field (e.g. Abell 1975). On the other hand, much work has been concerned to establish differences in the LF as a function of cluster morphology. Indeed, a universal LF is hard to explain theoretically. For example, according to the cannibalism line of argument (e.g. Hausman & Ostriker 1978), cD galaxies grow at the expense of other fainter galaxies – thus such a model predicts a deficit of bright galaxies in the most dynamically evolved clusters. The brightness of the first-ranked cluster galaxy is thus related to the dynamical state of the cluster, and the LF is expected to correlate with the

★E-mail: sll@aaoepp.aao.gov.au (SLL); v.r.eke@durham.ac.uk (VRE); cac@staru1.livjm.ac.uk (CAC); nichol@astro.phys.cmu.edu (RCN); guzzo@astmim.mi.astro.it (LG)

Bautz–Morgan (B–M) type, as this measures the contrast of the first-ranked galaxy compared to the other bright galaxies. Such a deficit in bright galaxies is also expected if tidal stripping in the outer haloes of galaxies, due to interactions, is taking place (Richstone 1975, 1976; Merritt 1983; Malumuth & Richstone 1984). Only in the special case in which the luminosity function is determined during the formation period of the cluster, with little further dynamical evolution taking place, are no correlations of the LF with other cluster properties expected (Merritt 1984, 1985).

The most popular approach taken to the study of the LF is to fit Schechter's (1976) parametrized form, given by

$$n(L)\,\mathrm{d}L = n^*(L/L^*)^{\alpha}\exp(-L/L^*)\,\mathrm{d}(L/L^*),$$

where n^* is a normalization factor, α is the power-law slope at the faint end, and L^* (or equivalently M^*) is the characteristic luminosity (magnitude). Schechter (1976) determined the best-fitting parameter values to be $M^* = -21.41$ (J band) and $\alpha = -1.25$. In subsequent studies there has been claim and counter-claim regarding the properties of this function. In a study of 12 very rich clusters, Dresler (1978) concluded that M^* does vary significantly from cluster to cluster and that it is correlated with the absolute magnitude of the first-ranked galaxy, in the sense consistent with the trend expected in the cannibalism model. Lugger (1986) studied a sample of nine Abell clusters and concluded that, while the mean values of M^* and α are in good agreement with those of Dressler (1978) and Schechter (1976), there was no evidence for a correlation of M^* with cluster morphology, central density or magnitude of the first-ranked galaxy. The examination of a further 14 rich clusters by Colless (1989) draws very much the same conclusions as Lugger (1986), with no variation in the cluster LFs with B–M type or richness seen. Simulations suggest that variations of more than 0.4 mag in M^* or 0.15 in α are ruled out by these data. Colless did find a marginally significant result such that the LF of the high-velocity dispersion clusters has fainter M^* compared with the low-velocity cases.

There are potential criticisms of these previous studies: first, as pointed out by Lugger (1986), the early studies such as that of Dressler (1978) did not use a consistent cluster radius or limiting absolute magnitude in comparing different cluster LFs. Secondly, the best previous studies (those of Dressler 1978, Lugger 1986 and Colless 1989) confine their selection to Abell clusters, and typically only the richer examples of these systems. Since there are potential systematic biases in the way in which Abell clusters were selected (for example, cD dominated clusters are much easier to detect by eye), these studies cannot necessarily be held to be a true reflection of the properties of all clusters. Finally, previous studies have relied on global number counts to correct for the non-cluster background present, and have used counts often taken in different passbands and from different surveys. This can lead to systematic errors due to differences in the calibrations of the data the LF is derived from and the data the counts are taken from.

Here we have re-examined the LF afresh using a sample of 46 clusters, selected automatically from digitized data. As a result this study has certain advantages over previous work in the field. The clusters are selected from photometrically calibrated digitized scans of photographic plates using an automatic search algorithm (hence our data should be more uniform than the Abell catalogue). The sample covers a wide range of richness and many of the clusters have well-determined velocity dispersions, allowing us to test for variations in the LF as a function of intrinsic cluster properties.

2 THE CLUSTER SAMPLE

2.1 The catalogue and the redshift survey

The sample of clusters used in this paper is drawn from the Edinburgh–Durham Cluster Catalogue (hereafter EDCC: Lumsden et al. 1992), which in its turn is derived from the Edinburgh–Durham Southern Galaxy Catalogue (hereafter EDSGC: e.g. Heydon-Dumbleton et al. 1989). The EDSGC consists of digitized COSMOS scans of 60 UK Schmidt Telescope III-aJ survey plates centred on the South Galactic Pole, and is nominally 95 per cent complete to $b_j = 20$ with less than 10 per cent contamination. A cluster sample was derived from the galaxy data in the EDSGC as outlined in Lumsden et al. There are over 700 potential clusters in the EDCC, and this sample is the first published machine-based cluster sample. The objective nature of the construction of the EDCC implies that it does not suffer from the systematic subjective biases that appear in the southern extension of the Abell catalogue covering the same area (Abell, Corwin & Olowin 1989). The EDCC is complete within its selection criteria to a limiting magnitude for the tenth-ranked cluster member of $b_j = 18.75$.

For a smaller sub-sample of the EDCC clusters, we obtained redshifts with the multi-slit spectrograph EFOSC on the ESO 3.6-m and with the multi-fibre spectrograph Autofib at the 3.9-m Anglo-Australian Telescope. The nature of this sample is discussed in Nichol et al. (1992) and Guzzo et al. (1992) and the redshifts are published in Collins et al. (1995). Approximately 10 per cent of those clusters observed proved to have significant contamination from other groups along the line of sight at significantly different redshifts. We have excluded those clusters with 'projection effects', as defined by Collins et al. (1995), from our sample. We note that the remaining clusters do not have a well-defined cut-off cluster richness (unlike the sample of Nichol et al. 1992), since we have included all the clusters for which we actually obtained redshifts.

From this data set, we have excluded those clusters in which the cluster background radius (as defined in Section 3.3) overlaps the boundaries of the EDSGC for ease of computation, and those clusters where their respective Abell radii are entirely superposed, since there is no well-defined cluster magnitude distribution. We also individually checked all the other clusters where the Abell radii of the two clusters overlapped, since the deblending procedure described in Lumsden et al. (1992) can occasionally cause the derived cluster centroid to move away from the 'true' position. We removed those clusters where the catalogue positions differed from both the centre derived from a visual inspection of the plate and the centroid of those galaxies for which we have redshifts by a significant fraction ($\sim$30 per cent) of the Abell radius. For blended clusters that pass this test, we assign galaxy membership to the individual clusters using the method described in Lumsden et al. (1992). Lastly, to be confident that we have removed all

clusters that may have contaminating projection effects, we chose to use only those with a minimum of four cluster redshifts, and where the number of galaxies with redshifts outside of the cluster is less than the actual number of bona fide cluster members.

The parameters of the remaining 46 clusters (as taken from Lumsden et al. 1992 and Collins et al. 1995) are given in Table 1. For all of the clusters, we have considered cluster members to be those galaxies within one Abell radius (where we have taken $r_A = 1.5\,h^{-1}$ Mpc, and we use the value for the Hubble constant $h = 1$ throughout[1]). Our sample is the largest single data base of clusters which has been used to study the LF to date.

2.2 Magnitude calibration

The EDSGC was calibrated from photometric CCD sequences assuming that the plate and CCD magnitudes were linearly related (Heydon-Dumbleton et al. 1989). However, for bright objects whose profiles are either strongly peaked (such as elliptical galaxies) or stellar, there is a regime in which the measured COSMOS magnitude is less than the true magnitude, caused by lack of dynamic range within the measuring machine itself. This 'saturation' occurs for elliptical galaxies at $b_j \sim 17$ (note that the plates themselves only saturate at much brighter magnitudes). Fainter than this magnitude, and for most late-type galaxies, the original calibration is correct, so that previously published results from the EDSGC are unchanged by these corrections. However, since most clusters are dominated by elliptical galaxies at the bright end of the LF, it is vital that we correct for this effect or else we will induce errors in the measured value of the 'break' in the LF for the nearby clusters.

We have calculated a correction for this effect, by comparing the catalogued EDSGC magnitude against the observed magnitude for 451 galaxies present in the CCD sequences used to calibrate the EDSGC initially (Heydon-Dumbleton et al. 1989). Since for faint magnitudes the slope should be linear, but at bright magnitudes it should diverge from this, we used a quadratic fit to the data. From this we derive a fit with the form (see Fig. 1)

$$b_j(\mathrm{EDSGC}) - b_j(\mathrm{CCD}) = (1.06 \pm 0.26) \times 10^{-2} b_j(\mathrm{EDSGC})^2 - (0.46 \pm 0.09) b_j(\mathrm{EDSGC}) + (4.96 \pm 0.90).$$

This fit should be reliable in the range $15 < b_j < 21$. For most of this range, the linear component present is actually the most important. This slope has been commented on previously by Heydon-Dumbleton (1989), and gives rise to the observed slope in the fit at fainter magnitudes, and is a result of the definition of measured photographic magnitude used in the EDSGC. As can be seen, the effect is small (the overall effect on the composite LF described in Section 5.1, for example, is 0.2 mag). However, for the purposes of the LF, we include all terms, so that our magnitude scale is more closely matched to the CCD-based magnitude scale.

It should be noted that this correction is an average, and may not represent every cluster absolutely. Since the saturation effect is a function of the photographic density, anything else that modifies this (such as vignetting, emulsion flaws, plate fogging or emulsion desensitization near the plate corners) will consequently affect the amount of saturation present. We do not have sufficient CCD sequences to map these effects fully; however, we note that the overall photographic intensity–magnitude relation has been corrected for these effects (see Heydon-Dumbleton 1989). These effects may in part give rise to the observed scatter in Fig. 1. We expect the magnitude of any error caused by using this average calibration to be small, since the deviations from the fit are small.

3 THE CLUSTER GALAXY LUMINOSITY FUNCTION

3.1 Form of the luminosity function

As is common with studies of the cluster galaxy luminosity function, we use the standard Schechter function (Schechter 1976) as the analytical model for our data. This function has the following form when expressed in terms of absolute magnitude:

$$n(M)\,\mathrm{d}M = kn^* \times \exp\{k(\alpha+1)(M^*-M) - \exp[k(M^*-M)]\}\,\mathrm{d}M, \quad (1)$$

where $k = \ln 10/2.5$. Here M is the absolute magnitude, derived from the measured apparent magnitude m using

$$M = m - 42.384 + 5\log h - 5\log z - K(z) - A(b_j),$$

where $K(z) = 4.14z - 0.44z^2$ is the K-correction suitable for the b_j passband for the mix of galaxies typically observed in low-redshift clusters (Ellis 1983), and $A(b_j)$ is the effective extinction in this passband. This latter quantity is derived using techniques described in Nichol & Collins (1993) for each cluster. In common with other studies of the luminosity function, we assume that $q_0 = 1$ in deriving the distance modulus used, and we have adopted $h = 1$ for simplicity as well. The LF normalization n^* is constrained using the actual observed number of cluster galaxies, and we carry out either a two-parameter fit to M^* (the absolute magnitude of the 'break' in the LF) and α (the exponent of the power-law slope at fainter magnitudes), or a one-parameter fit to M^* with α fixed where required.

3.2 The composite luminosity function

There are too few galaxies per bin in the individual LFs to fit both M^* and α simultaneously. Since we wish to search for deviations from some 'mean' LF, it is valuable to consider co-adding all the LF data into an average or composite luminosity function, in a way that allows us to estimate both parameters simultaneously. The easiest manner in which to do this is to consider the composite luminosity function defined by Colless (1989) to be

$$N_{cj} = \frac{R_c}{n_{\mathrm{clus},j}} \Sigma_{\mathrm{clus}} \frac{N_{ij}}{R_i}, \quad (2)$$

where R_i is the 'richness' of the ith cluster, $n_{\mathrm{clus},j}$ is the number of clusters that actually contribute to the jth bin of the composite LF, N_{ij} is the background corrected number

[1]Where $h = H_0/100$, and H_0 is the Hubble constant in units of km s^{-1} Mpc^{-1}.

Table 1. The full cluster sample. The EDCC number refers to the identification in Lumsden et al. (1992). The field is the original Schmidt J survey field number. N_{tot} is the actual number of redshifts obtained for that cluster, and N_{clus} is the number of those redshifts adjudged to lie in the cluster. BM class is the Bautz-Morgan class, where 1 represents class I, 3 represents class II, 2 represents any other defined class and 0 implies that the cluster concerned is not in the Abell et al. (1989) catalogue and therefore has not been classified. The velocity dispersion is taken directly from Collins et al. (1995).

EDCC	RA			Dec			Field	Redshift	N_{tot}	N_{clus}	BM class	Vel. Disp. (km/s)
42	21	46	21.9	-30	56	37.8	466	0.11949	8	4	2	
51	21	49	22.2	-29	8	1.7	466	0.0927	6	5	0	
61	21	53	59.4	-30	19	37.8	466	0.09257	4	4	0	
124	22	14	43.9	-35	57	33.1	405	0.14661	10	9	2	1011
131	22	16	39.2	-34	56	27	405	0.15711	4	4	3	
145	22	24	56.7	-30	51	11	467	0.05697	12	11	2	1105
261	23	9	9.4	-29	19	41.1	469	0.11709	8	6	1	820
311	23	28	36	-36	47	41.4	408	0.09544	7	5	1	
348	23	44	33.7	-28	31	40.6	471	0.0292	33	32	3	830
366	23	52	19.6	-27	56	40	471	0.07278	8	6	3	464
392	0	0	13.9	-34	56	38.4	349	0.11272	8	7	3	525
394	0	0	32.1	-36	12	58.9	349	0.04902	6	6	1	598
400	0	3	39.1	-34	58	49.1	349	0.11307	10	7	2	1222
408	0	7	27.8	-35	56	8.6	349	0.11936	14	13	2	871
421	0	13	35.9	-35	13	53.1	350	0.14618	7	5	3	
429	0	15	23.2	-35	25	2.5	350	0.09693	19	17	3	790
437	0	18	1.2	-25	54	26.3	473	0.1432	6	5	1	
438	0	20	23.5	-38	24	12.6	294	0.11919	4	4	2	
450	0	27	23.4	-29	45	1.3	410	0.0988	5	4	3	
460	0	34	47.1	-28	44	47.4	411	0.1122	31	21	1	700
462	0	35	14.4	-39	23	42.4	294	0.06316	12	11	1	569
470	0	37	26.4	-26	26	25.1	474	0.10975	10	7	0	415
471	0	37	43.3	-24	56	48.3	474	0.11175	7	4	3	
473	0	40	3.7	-28	50	23.2	411	0.10799	14	13	1	695
474	0	40	44.7	-26	19	53.9	474	0.11256	15	8	3	354
482	0	46	50.3	-29	47	22	411	0.10783	30	21	1	675
485	0	48	56.3	-28	46	50.4	411	0.11251	6	6	2	443
495	0	53	28.6	-26	36	9.4	474	0.11412	17	14	3	403
499	0	53	51.4	-38	10	2.1	295	0.11697	4	4	3	
519	1	2	7.7	-40	6	22.4	295	0.1073	13	9	1	371
524	1	5	39.9	-37	1	20.6	352	0.11751	9	9	1	975
553	1	23	9	-39	41	37.1	296	0.08791	14	12	1	242
557	1	23	46.9	-38	14	34.8	296	0.07969	8	6	1	413
575	1	31	52.4	-27	47	19.3	476	0.12545	7	5	1	
606	1	58	27.2	-33	11	15.2	354	0.10045	12	11	3	1152
653	2	27	16.9	-33	41	37	355	0.07924	6	6	0	440
658	2	28	34.9	-33	17	55.5	355	0.07636	26	22	3	977
683	2	42	26.6	-26	31	10.7	479	0.13364	4	4	3	
699	2	49	17.9	-25	9	1.2	480	0.11113	7	6	2	891
712	2	54	19.6	-24	55	51.1	480	0.11093	19	13	1	519
722	3	1	3.9	-37	7	47.2	357	0.06664	4	4	1	
726	3	4	43	-39	1	47.3	300	0.08737	4	4	0	
728	3	6	13.3	-36	53	32.2	357	0.06748	9	8	1	323
735	3	9	23.7	-27	5	34.3	481	0.06826	9	7	1	359
742	3	11	52.2	-38	30	34.7	300	0.08384	6	6	1	709
748	3	13	9.5	-29	24	14.2	417	0.06709	6	5	2	

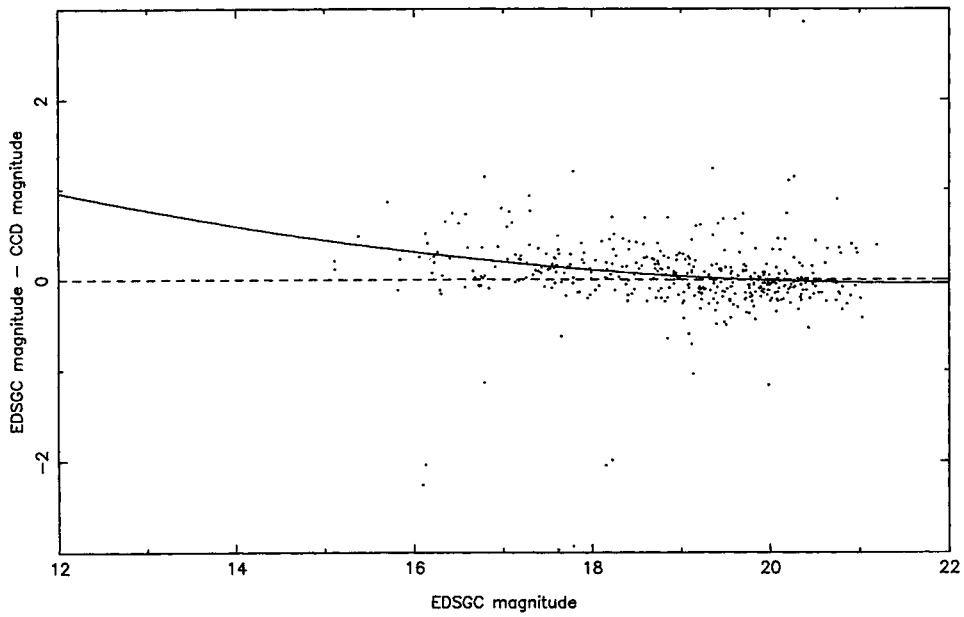

Figure 1. The relationship between the catalogued EDSGC b_j magnitude and the derived b_j magnitude from the CCD sequence. The solid line represents the best-fitting quadratic given in the text. The dashed line is given as a guide to the eye to show the deviation between the CCD magnitude scale and the EDSGC scale.

of galaxies in the jth bin of the ith cluster's LF and $R_c = \Sigma_{clus} R_i$. We use a different definition of R_i from that of Colless, since he used the total number of galaxies brighter than $M = -19$ and we use the background-corrected number of cluster galaxies between $M(b_j) = -19.5$ and $M(b_j) = -20.5$. This is because our sample contains more distant clusters on average than the Colless sample, and we would otherwise discard a significant fraction of the data as being objects where $M = -19$ was beyond our chosen completeness limit. We also impose an upper limit in absolute magnitude when calculating the richness to avoid the problems with very bright galaxies discussed above. For typical values for the LF ($M^* = -20$ and $\alpha = -1.25$), the relationship between our definition of richness and that of Colless is $R_i(\text{Colless}) \sim 2R_i(\text{here})$.

Similarly, the errors for the composite LF are calculated according to

$$\delta N_{cj} = \frac{R_c}{n_{clus,j}} \left[\Sigma_{clus} \left(\frac{\delta N_{ij}}{R_i} \right)^2 \right]^{1/2}, \quad (3)$$

where the δN_{ij} are derived according to the error given in Section 3.4.

3.3 Background galaxies

In order to derive the LF, we must be able to define the expected contribution from background galaxies, n_{back}, accurately. We have considered three approaches to this problem. First, we used the counts in an annulus, centred on the cluster, with an inner radius of one degree and a width of one degree. This fixed radius was adopted for simplicity – using a fixed metric radius as opposed to a fixed angular radius gives essentially the same results. This method has the advantage that the correction is strictly local, and hence the variation in field counts seen in different regions of the EDSGC is correctly accounted for. For the other two methods, we used the global counts as derived from the whole of the EDSGC, and the average of the counts from the annuli from the first method described above. The first of these is similar to the procedure used in previous studies, but since our global counts actually come from the same data the LFs themselves are constructed from, we remove the possibility of errors arising from discrepancies in the calibration of the LF and the global counts. The second has the potential advantage that it excludes the rich clusters from the counts and hence is a better measure of the 'true' background. In Fig. 2 we show the derived counts from the catalogue as a whole, together with the average of the counts derived from the annuli around the clusters. There is essentially little difference between these *on average*. The difference that does exist is at the level expected from the presence of real large-scale structure. There is little sign that excluding the cores of the rich clusters makes the background as calculated from the annuli lower than the global counts.

Previous estimates of the background count for use in the LF have been derived from either separate 'eyeball' galaxy catalogues (e.g. Dressler 1978, Lugger 1986) or have been based on data from only very small areas (Colless 1989). We note in passing that the slope of the number counts that we find is larger than that assumed in previous studies of the LF. This is, however, consistent with Maddox et al. (1990), the only other measure of the counts over significantly large areas of the sky that is derived using a measuring machine. The fit given by Colless (1989) appears to overcount the true background by ~ 20 per cent.

Lastly, we note that the derived number counts shown in Fig. 2 drop off more rapidly than $m^{0.45}$ at $b_j > 20$. This disagrees with other observations (e.g. the deep CCD counts presented in Metcalfe et al. 1991), and indicates that the overall completeness limit of the EDSGC is $b_j \sim 20$. How-

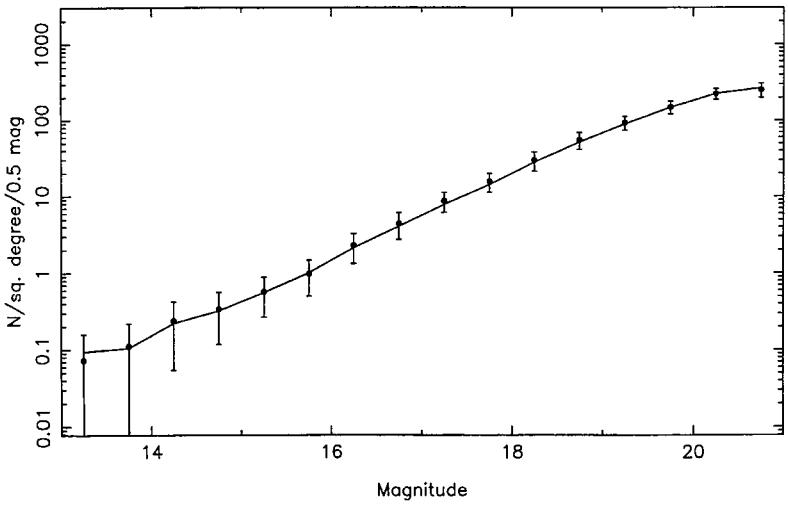

Figure 2. The number counts from the EDSGC derived from the whole catalogue (the solid line), and from the average of all the annuli used for background correction of the LF (●). The difference between the two never exceeds 10 per cent. The error bars shown represent the variance of the counts derived from the annuli.

ever, inspection of the number counts on individual Schmidt plates also shows that this limit varies from plate to plate. We have allowed for a possible variable completeness with plates in our work by examining the number counts on each plate separately and assigning completeness limits relative to the seven deepest fields in the survey. From this we find that the best plates are complete to $b_j = 21$ and the worst to $b_j = 19.5$. We do not, however, use data fainter than $b_j = 20$ from any field. For those fields where the adopted completenesss limit is brighter than this, we do not use data fainter than that limit. In calculating the background correction required when using the global number counts we have interpolated the actual measured data, rather than fitting a single power law. The latter is a poor representation to the actual data, since the true number counts 'turn-over' near $b_j \sim 19$ (e.g. Metcalfe et al. 1991). This regime is important for our work since for clusters with $z \sim 0.1$, $b_j = 20$ is equivalent to an absolute magnitude of ~ -18.

We also have to derive suitable error estimates for these background counts. There are two sources of error, which are presented in all the methods given above. The first is simply the Poisson uncertainty in the counts and can be represented simply as $\sqrt{n_{\rm back}}$. The second is systematic and represents the presence of large-scale clustering within the sample. For the gobal correction method, although we would assume that the slope of the background number counts is constant over the survey region, the normalization of these counts changes with position. Colless (1989) and Lugger (1986) follow Geller & Beers (1982) in assuming that the background is only known to 50 per cent. For the background derived from the local annuli we can estimate the error rather more accurately, however. If we take all of these annuli, and find the scatter about the mean of the number counts, then we can derive the systematic error for this method. Since all the annuli have the same area, any number density deviations are purely due to the presence of large-scale structure. The derived variance is also shown in Fig. 2. Comparison of the expected contribution from Poisson error and the total error observed indicates that the mean field-to-field variance is 25 per cent for $b_j > 17$. The largest excursions seen are < 50 per cent over the same magnitude range. Therefore, using the 50 per cent variation in what follows, although conservative, does account for all the observed variations, whereas using the 25 per cent mean variation is a better representation of the data as a whole but will underestimate the error in the background for a few clusters. We demonstrate in Section 5.1 the effect of using this smaller error on the field counts compared to the value favoured by Geller & Beers (1982). We note that Dressler (1978) also found that a mean variation of 25 per cent was a good fit to his data, and this result is compatible with the known angular clustering in the EDSGC (Collins, Nichol & Lumsden 1992).

3.4 Fitting methods

We have considered only a χ^2 fitting method in deriving the parameters M^* and α. If we let $n_{\rm clus}$ be the difference between the total counts in a bin and the expected background in the bin (however the latter is calculated), so that

$$n_{\rm clus} = n_{\rm tot} - n_{\rm back},$$

then we seek to minimize the function

$$\chi^2 = \Sigma \frac{(n_{\rm clus} - n_{\rm fit})^2}{\sigma(n_{\rm fit})^2}, \qquad (4)$$

where

$$n_{\rm fit} = n(M)\Delta M + \frac{n''(M)\Delta M^3}{24.0}$$

and

$$\sigma(n_{\rm fit}) = [\sigma(n_{\rm tot})^2 + \sigma(n_{\rm back})^2]^{1/2}.$$

Throughout we use a bin width, ΔM, of 0.5 mag. The presence of the second derivative in the form of $n_{\rm fit}$ takes account of the finite bin width used, since the number counts change extremely rapidly (Schechter 1976). The first

term in the error represents the Poissonian error in the total observed counts. Therefore, $\sigma(n_{\rm tot}) = n_{\rm tot}^{1/2}$. The second term must take account of both Poissonian error and systematic errors in the background as noted in Section 3.3. This has the form $\sigma(n_{\rm back}) = \max(n_{\rm back}^{1/2}, xn_{\rm back})$, where $x = 0.5$ (except where explicitly noted that $x = 0.25$).

Although for many of the clusters data exists with M brighter than -21 and fainter than -18, there are good reasons for not using such data in deriving values of M^* and α. First, for the fainter galaxies, the correction for the background becomes more difficult since the background fraction per bin rises steadily. For any given cluster we impose two limits on this: (1) that any data with $m(b_j) > 20$ be discarded, for reasons outlined in Section 3.3, and (2) that any bin for which the number of background galaxies exceeds the cluster galaxies also be discarded. In practice, the former limit essentially ensures the latter for faint galaxies in any event. For bright galaxies there are also problems we wish to avoid. It is desirable, as has been noted previously (by, e.g., Lugger), to exclude the brightest cluster galaxy when deriving the LF. We automatically do this since we discard all galaxies brighter than $M = -21$ (typically of order five galaxies in the richer clusters). There are more specific reasons for doing this in our case as well. First, the saturation correction is poorly defined brighter than $b_j = 15$, and hence the magnitudes of the galaxies brighter than this are likely to have larger errors. At $z = 0.05$, this magnitude corresponds to $M = -21.5$, and at $z = 0.1$, $M = -23$. Therefore, it is clear that galaxies brighter than $M = -21$ should not be used because their photometry is suspect. Secondly, COSMOS data is deblended where object mergers occur (cf. the discussion in Lumsden et al. 1992), but the accuracy of the magnitudes of the deblended data is less reliable than for single isolated objects. The brightest galaxies in clusters are almost always blended with fainter satellite systems in the EDSGC data, so again the photometry of these objects is not reliable. Discarding the brightest bins of the LF guards against problems of this kind. It is possible that similar problems may also be present in previous derivations of the LF, since the work described in the Introduction also relied extensively on photographic plate material. In any event, we recommended that results which rely on accurate magnitudes for the brightest galaxies in any LF derived from photographic plates should be treated with caution. We have also placed constraints on the values of M^* and α that the fitting routine can accept, to prevent any possibility of the fitting process 'running away'. These limits are that M^* should lie between -18 and -26 and that α should lie between 0 and -2.5. Therefore, quoted values for the fits that are near these limits are indicative of a very shallow minimum in the fit, and hence that the reliability of the fit is likely to be low (whatever the quoted formal probability that the fit is good). Finally, we note that we sum bins to ensure that there are ≥ 5 galaxies per bin in the data being fitted, as is standard for χ^2 minimization techniques.

4 RELIABILITY OF THE FITTING PROCEDURE

Before we can consider the actual data, we need some estimate of the reliability of our fitting procedure and the true error on these fits. To achieve this, we conducted extensive Monte Carlo simulations. In particular, we carried out three sets of simulations: first, to estimate the effect that errors in the assumed background had on the fit parameters as a function of redshift; secondly, to derive a measure of the true error distribution for a one-parameter fit to a model LF as a function of richness, for R_i typical of the single cluster values we found; and finally, to derive the error distribution for the two-parameter fits to the composite sets. These latter two will then allow us to estimate the true likelihood that observed departures from the composite LF are in fact truly significant. In carrying out these simulations, we have assumed that $M^* = -20.2$ and $\alpha = -1.25$ for the model of the LF (in accordance with the results derived in Section 5.1).

In order to check the effect of the background subtraction alone, we initially assumed that the form of the LF was known perfectly, and only the background was allowed to vary. We used the global background as derived above, and rescaled it at random so that the variance was 25 per cent as was found to be the case in practise in Section 3.3. Thus after normal background correction, the random LF would have either too many or too few background galaxies subtracted. By deriving fit parameters for many such data sets, we can derive the average error induced in those parameters as a function of cluster richness and redshift. In general, for $z < 0.05$, the effect of errors in the background on the fit parameters is negligible, even for poor clusters. At high redshifts, M^* can be measured to an accuracy of 0.05 mag if $R_i > 30$ (i.e. the average of the measured M^* from the simulations is different by this amount from the assumed input M^*). At $z > 0.05$ and $R_i < 20$, the scatter in the derived value of M^* becomes larger (~ 0.5–1.0 mag). The values derived here should be the dominant source of error when the richness is very large (since then the LF is known almost perfectly). Since the composite luminosity functions given all have effective values of the richness that are much greater than 100, it is clear that the empirically derived errors for the effect of different background corrections given in Section 5.1 are in good agreement with the results of these Monte Carlo simulations.

More generally, we need to map out true estimates of the likely scatter in the fits to M^* when the LF was drawn at random from the same model LF used above. In this case, since we draw individual galaxies at random from the parent LF, we also include random fluctuations in the LF itself. For low- to moderate-richness clusters, it is these fluctuations that dominate the scatter in the fits to M^* rather than the background correction method. Although the resultant values are therefore independent of redshift, we have adopted $z = 0.1$ as typical of our clusters, in order to include a suitable background contribution. This background is derived in the same manner as described above. Table 2 gives the limits outside of which 90, 31.5, 10, 5 and 1 per cent, respectively, of the data lie. One of the most noticeable features of these simulations is that the distribution of fitted values of M^* is skew, with a strong tail towards brighter magnitudes. An example of this is shown in Fig. 3, where we present the distribution of fits to M^* for two richnesses, $R_i = 10$ and $R_i = 50$. This trend is due to the restricted range of absolute magnitudes that are actually used to fit against. Since we set $M^* = -20.2$ in accordance with the result we find in Section 5.1, there are only two bins

Table 2. The measured distribution of the fitted values of M^* as a function of richness from Monte Carlo simulations. The percentage values listed refer to the values of M that exclude that fraction of the actual measured fits. Since the distribution is skew, two limits are given for each percentage. A * implies that no acceptable fits could be found ($M^* < -26$) for that fraction of the data. The last row gives the results for a simulation in which data was fitted over the range -23 to -18, showing the effect that the truncation at the bright end of the LF has on the fitting process.

R_i	90%		31.5%		10%		5%		1%	
200	−20.21	−20.18	−20.32	−20.09	−20.41	−20.03	−20.45	−20.01	−20.56	−19.95
50	−20.24	−20.18	−20.49	−19.98	−20.74	−19.87	−20.89	−19.82	−21.36	−19.74
40	−20.24	−20.16	−20.57	−19.95	−20.90	−19.83	−21.17	−19.76	−22.00	−19.65
35	−20.25	−20.17	−20.60	−19.95	−20.91	−19.83	−21.22	−19.75	−22.31	−19.62
30	−20.28	−20.19	−20.68	−19.94	−21.19	−19.78	−21.70	−19.74	*	−19.59
25	−20.29	−20.17	−20.79	−19.87	−21.55	−19.71	−21.99	−19.63	*	−19.50
20	−20.32	−20.19	−21.06	−19.88	−22.71	−19.73	*	−19.62	*	−19.51
15	−20.35	−20.18	−21.32	−19.84	−25.94	−19.62	*	−19.55	*	−19.14
10	−20.35	−20.18	−21.39	−19.75	*	−19.45	*	−19.34	*	−19.04
25	−20.23	−20.17	−20.52	−20.00	−20.88	−19.88	−21.11	−19.83	−21.73	−19.70

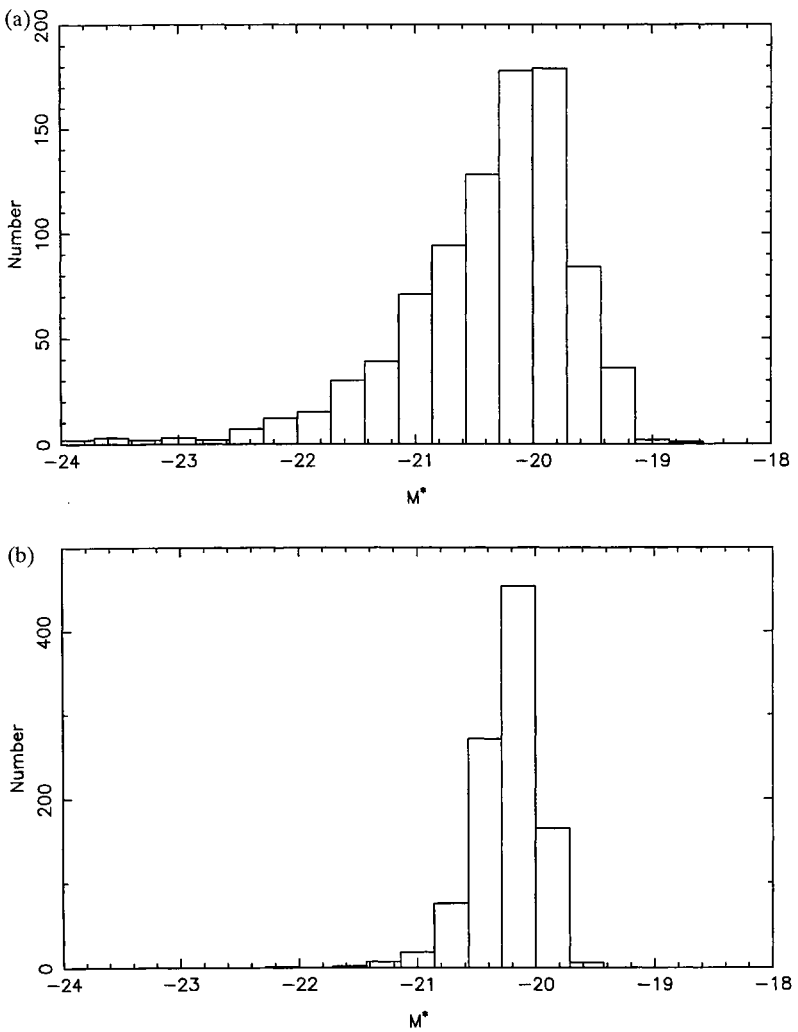

Figure 3. Derived values of M^* from one-parameter fits to model Schechter luminosity functions for clusters with (a) $R_i = 10$ and (b) $R_i = 50$, when the fit is over the range $-18 > M > -21$. The model LF has $M^* = -20.2$ and $\alpha = -1.25$. When this range is extended to $-18 > M > -23$, the distribution of M^* for $R_i = 25$ is given in (c). This is clearly similar to the higher richness distribution when fitted over the narrower range in absolute magnitude.

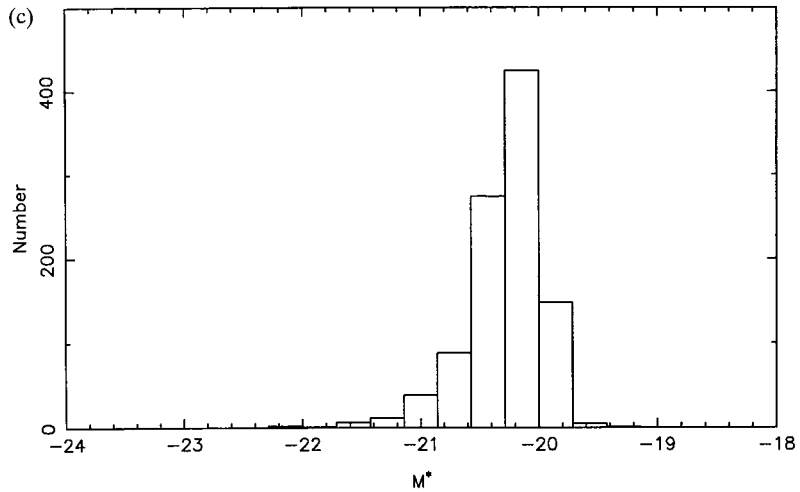

Figure 3 – *continued*

in the fitted LF that actually sample the break. At low-richness values there are often insufficient counts per bin to truly define this break, and hence, since there is no constraint from the actual data, the fitted value of M^* can take quite large negative values without changing the χ^2 of the fit significantly. In practice, the limit for M^* at the bright end is set by our constraint that $M^* > -26$. Clearly, for the richer sample shown in Fig. 3 the trend towards a strongly skewed distribution is much less evident, as expected. This skewness also shows in the mean M^* derived from the simulations, with this value being the input value of -20.2 at large richness but diverging to -20.8 at $R_i = 10$. This same behaviour is also demonstrated (in a slightly different fashion) by the simulations of Colless (1989), where he shows that the probability that a two-sample χ^2 test can reject the possibility that two clusters are drawn from the same underlying population is also skew with respect to M^*. We can further confirm the reason for this skewed distribution, by looking at the distribution of M^* when the absolute magnitude range being fitted is -23 to -18. The results for $R_i = 25$ are given in Table 2 and also shown in Fig. 3. It is easy to see the effect that including the brighter galaxies has on fixing the location of the break in the LF. The slight skewness left in the distribution now reflects the fact that the total number of galaxies with $M < -21$ in these low-richness systems is rather small. The derived error bounds including these bright galaxies are most similar to those for a much higher value of R_i (~ 40) when fitted over the normal range in M. The key result of these simulations, therefore, is that it is difficult to rule against overly bright values of M^* as being from the same distribution as the composite. However, those clusters for which M^* is rather fainter than the composite are strongly discriminated against. We note that the results of these simulations can also be applied to the data of Colless (1989), and that the simulations of Dressler (1978) are not applicable to the case of fitting over a restricted magnitude range (or rather that the Dressler results would be closer to those achieved in practice but for a much larger true richness).

It is worth also considering how sensitive these results are to our assumed value of α. We tested this using $\alpha = 1.2$ for $R_i \sim 20$, typical of our sample. We found that the changes are small (< 0.1 in the faint limit on M^*, and < 0.2 in the faint bright limit) and always act to push these limits *brighter*. Since the cluster LFs we can exclude are those which have faint M^*, it is clear that adopting a lower value of α will only make this difference larger. The formal average of our composites using all methods of calculating them give $\alpha = -1.22$ (Table 3). This implies that the probability that any LF agrees with the derived composite as given by the simulations is slightly conservative.

Since we have carried out two-parameter fits in Sections 5.1 and 5.3, we also need to know the likely joint distribution of α and M^* for the case of rich systems alone (i.e. composite LFs). We therefore carried out simulations as described above, but in this case applied a two-parameter fit to the LF. In this instance the best way to present the data is graphically, and the results of the simulations are shown in Fig. 4. The contour levels plotted correspond to the same probabilities given for the one-parameter case in Table 2. The simulations have been binned into 0.05 in α and 0.1 in M^* for presentation.

It is clear from Fig. 4 that M^* and α are highly correlated. In what follows we will present formal error estimates on each fit, derived by determining the value(s) at which $\chi^2 = \chi^2_{\rm min} + 1$. As will be seen, there is a considerable difference between these formal errors and both the error distributions given in Table 2 for the one-parameter fits and the distribution shown in Fig. 4 for the two-parameter fits. This difference largely stems from the correlation between M^* and α, since the errors in these are also therefore clearly correlated. These formal errors are included for completeness only (since they do provide a measure of 'goodness-of-fit'). We will only use the Monte Carlo simulations and two-sample χ^2 tests when assessing the true deviations that may be present between any given LF and a universal composite.

5 RESULTS

5.1 The composite luminosity function

The first LF we consider is the composite of all the clusters which have $R_i > 20$. There are 23 clusters in this sample, and

Table 3. Fits to the various composite LFs described in the text. The columns are: the description of the composite; the derived values of M^* and α (the error corresponds to the values of M^* and α where $\chi^2 = \chi^2_{\rm min} + 1$); the formal likelihood that the fit is good; the number of clusters used in constructing the composite; the derived value of n^*; and the measured richness of the composite.

Sample	M^*	α	p(fit)	n_{clus}	$n_{clus}n^*$	R_C
50% Background error						
Local background correction	-20.14 ± 0.01	-1.18 ± 0.01	92	23	1660	770
Global background correction	-20.19 ± 0.01	-1.25 ± 0.01	99	23	1620	810
Global correction using the annuli	-20.15 ± 0.01	-1.23 ± 0.01	97	23	1650	790
All galaxies in the range $-22 < M < -17.5$, local correction	-20.66 ± 0.07	-1.27 ± 0.03	2	23	970	770
25% Background error						
Local background correction	-20.09 ± 0.02	-1.16 ± 0.01	86	23	1750	770
Global background correction	-20.19 ± 0.01	-1.25 ± 0.01	97	23	1620	810
Global correction using the annuli	-20.14 ± 0.01	-1.22 ± 0.01	94	23	1670	790

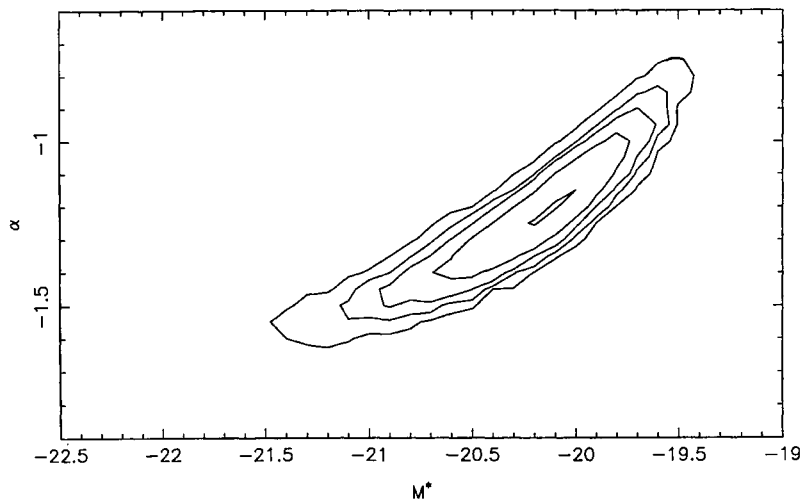

Figure 4. Contours of the derived distribution in M^* and α for 10 000 simulations of a two-parameter fit to the standard Schechter function. The initial model LF has $M^* = -20.2$ and $\alpha = -1.25$. The contours contain 10, 68.5, 90, 95 and 99 per cent of the data, respectively. The initial richness given to the model LF is $R_c = 250$, close to the measured value for most of our subsamples in Section 5.3. This is therefore the correct error map for comparison with the observed values of M^* and α from those composite subsamples.

the richness of the composite was found to be $R_c \sim 800$ ($n^* n_{\rm clus} \sim 1600$). This allows us to compare our results with previous samples which generally dealt with rich Abell clusters.

For this composite we have considered the effect of using the different background correction methods outlined in Section 3.3, as well as for the different assumed errors in that background subtraction. The results of the fitting process for these different background corrections are given in Table 3 and shown in Fig. 5.

The first three rows were derived by fitting both M^* and α to this sample over the magnitude range ($-21 \leq m \leq -18$) with an assumed field-to-field error in the background counts of 50 per cent. The first entry gives the results for the local correction method, the second for the global correction using all of the counts and the third the global correction but using only the average of the annuli around the clusters. Clearly the two global background corrections we have used give essentially the same result. Directly comparing the data derived from the local and global background correction methods using a two-sample χ^2 test also shows that these composites are in good agreement for the absolute magnitude range given above ($\gg 90$ per cent probability they are same). Moreover, since we have not renormalized the LFs before comparing using this test, this also indicates that differences that do exist between

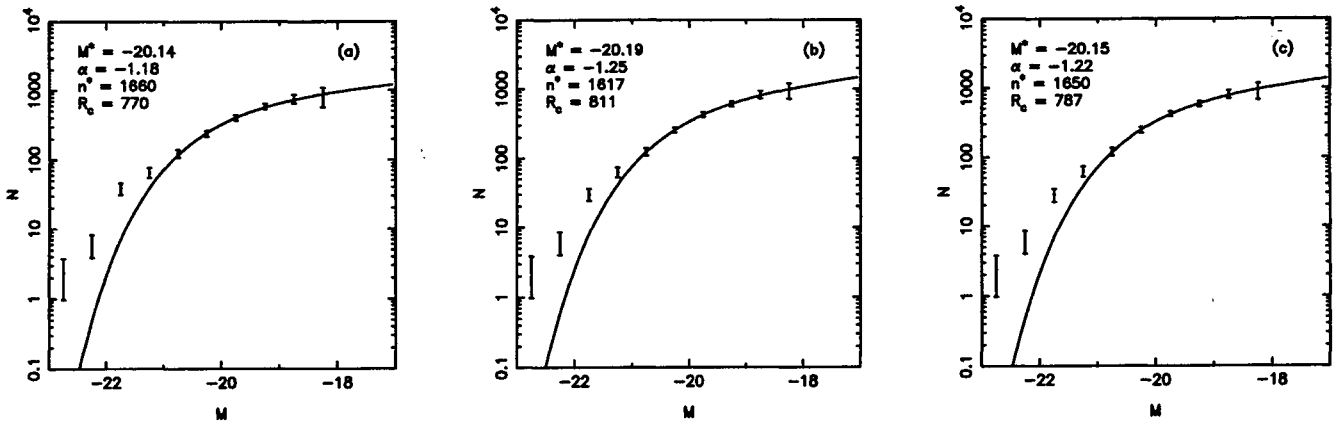

Figure 5. Measured luminosity functions for (a) the local background correction method, (b) the global background correction and (c) the global correction but using the average of the annuli from (a). The data are fitted to a Schechter function in the range $-21 < M < -18$. The best-fitting Schechter function is shown as a solid line. Only the data derived assuming a 50 per cent background variance are shown.

the background subtraction methods for individual clusters (as will be shown in Section 5.2) tend to average out when combined in the composite.

The last three rows in Table 3 give the equivalent results when the field-to-field background error is assumed to be 25 per cent, as noted in Section 3.3. This change therefore gives the same results as before within the derived errors on M^* and α for the global correction method, and only very slightly different in the formal sense for the local correction method. This shows that the dominant error in deriving estimates of M^* or α is actually the Poissonian contribution (cf. the discussion after equation 4), and that the variation due to assuming a different error on the background term alone is small. Indeed, the magnitude of the changes found here is negligible compared to the expected measurement errors as shown in Section 4. Henceforth, we consider only the 50 per cent field-to-field variation, since it adequately represents all of the clusters in the present sample.

Lastly, it is worth noting the effect that changing the magnitude range over which the fits are made has on these conclusions. Including the brighter galaxies pushes M^* brigher. Including the fainter galaxies makes a slight difference to the slope but little else. It should be noted, however, that only one cluster actually contributes for M fainter than -18, whereas all 23 clusters contribute at M brigher than -21. The result derived when the fit is over the range $-22 < M < -17.5$, using the local background correction, is also given in Table 3. The low probability that the fit is good is due to the fact that a Schechter function is now a poor fit to the data at both bright *and* faint magnitudes. We note that a similar (though larger) increase in brightness of M^* was found by Lugger when she considered mean luminosity functions with the brightest cluster galaxies included. However, we repeat our caution of Section 2.2 that data on such bright galaxies ($m < 15$) cannot be relied upon absolutely because of problems of saturation and image blending (cf. the discussion in Colless 1989). It is also not clear, therefore, whether or not the greater variance from the mean seen in the brightest bins, as compared to those in the more restricted absolute magnitude range over which we normally determine the LF, is actually real or merely an artefact of the COSMOS measurements.

5.2 Individual cluster luminosity functions

We also fitted each cluster LF separately to the Schechter function, but this time holding α constant (since there are insufficient points in many of the clusters to enable more than a one-parameter fit to be made successfully). We adopted $\alpha = -1.25$ as an appropriate compromise, based both on our own results and on those previously published. Table 4 shows the results of these tests for all 46 clusters that were found to have positive values of R_i, and Fig. 6 shows the actual data for those with $R_i \geq 15$. We quote results derived using both the global and local background-correction methods. We also tested for differences arising from the choice of background subtraction method by comparing the LF distributions directly. We used a two-sample χ^2 test to check for differences between the two sets of LFs, without rescaling the LFs for the possibility that the two background subtraction methods may have resulted in a different overall normalization. We have allowed for the fact that the adopted magnitude completion limit may be brighter than $M = -18$, so that we compare the LFs in the range -21 to the brighter of -18 or the plate completion limit. These limits are given in Table 4. The results of the two-sample χ^2 test are given in column 10 of Table 4. As can be seen the agreement is good, and even for the worst case (E748), we cannot rule out the possibility that the two samples represent the same underlying distribution.

We also compared the single cluster LFs with a suitably normalized model of the composite (assuming the average values of M^* and α found above), using a simple χ^2 test (given in Table 4), and with the results of the Monte Carlo simulations from Table 2. It can be seen that there are several clusters where the LF derived using global background subtraction is a poor match to the model, but the LF derived using the local background is a much better fit. We take this as evidence for the fact that assuming an overall global background will not be a good match to every cluster. Generally the two tests give similar results, though we note that the two-sample χ^2 test is considerably more conservative at ruling out individual LFs, as expected. However, all those LFs for which the two-sample χ^2 test gives a probability below 20 per cent are also found to be a poor match

Table 4. Best-fitting values of M^* for a one-parameter Schechter function fit to the individual cluster LFs. The error quoted corresponds to the mean of the deviations from M^* where $\chi^2 = \chi^2_{\min} + 1$. The probability quoted is the level at which this fit can be accepted. Both global and local background subtraction methods are given. For both of these the probability from a two-sample χ^2 test that the actual data differs from the composite LF is also given as p(CLF). Similarly, the probability that the local and global background subtracted data are the same is given as p(same). Lastly, the faint magnitude limit used in these tests is given. The bright limit is always -21.

EDCC	M^* (global)	p(fit)	R	p(CLF)	M^* (local)	p(fit)	R	p(CLF)	p(same)	M(faint)
42	-20.68 ± 0.18	70	61	47	-20.53 ± 0.24	85	49	85	99	-18.74
51	-20.60 ± 0.35	96	11	44	-20.71 ± 0.69	76	7	36	86	-18.07
61	-19.85 ± 0.16	24	33	21	-20.55 ± 0.36	89	25	95	98	-18.04
124	-19.94 ± 0.12	52	53	57	-19.95 ± 0.14	62	48	67	100	-18.90
131	-20.13 ± 0.20	94	37	99	-20.23 ± 0.23	95	36	100	99	-19.09
145	-20.42 ± 0.24	57	18	67	-20.42 ± 0.24	62	19	77	93	-18.00
261	-20.13 ± 0.22	23	25	34	-20.17 ± 0.21	24	28	39	98	-18.38
311	-20.67 ± 0.28	85	28	70	-20.70 ± 0.31	84	27	71	100	-18.00
348	-19.35 ± 0.15	73	10	9	-19.25 ± 0.19	74	8	15	99	-18.00
366	-20.45 ± 0.36	94	12	90	-19.92 ± 0.45	66	8	72	94	-18.00
392	-20.70 ± 0.26	95	29	90	-20.71 ± 0.43	99	22	98	100	-18.19
394	-19.74 ± 0.23	24	9	20	-20.18 ± 0.41	31	8	54	52	-18.00
400	-19.64 ± 0.11	62	39	8	-19.58 ± 0.14	70	33	19	100	-18.20
408	-20.40 ± 0.28	53	17	34	-21.42 ± 0.66	60	12	39	63	-18.35
421	-20.07 ± 0.18	64	36	80	-20.06 ± 0.22	62	31	81	98	-18.91
429	-19.47 ± 0.13	71	22	3	-19.55 ± 0.13	73	22	13	100	-18.00
437	-20.26 ± 0.16	97	53	99	-20.30 ± 0.15	99	56	99	100	-18.93
438	-19.49 ± 0.24	91	15	54	-19.47 ± 0.24	94	15	50	99	-18.57
450	-21.47 ± 0.53	50	18	45	-21.14 ± 0.51	72	18	78	83	-18.00
460	-20.56 ± 0.26	27	35	19	-20.33 ± 0.27	30	32	29	96	-18.73
462	-19.22 ± 0.27	69	9	51	-19.18 ± 0.20	49	10	23	100	-18.00
470	-20.93 ± 0.56	80	13	74	-19.68 ± 0.40	89	10	85	68	-18.35
471	-20.83 ± 0.34	98	26	83	-20.50 ± 0.32	97	24	96	98	-18.39
473	-20.52 ± 0.17	86	45	82	-20.32 ± 0.17	91	42	96	98	-18.63
474	-20.82 ± 0.37	22	23	30	-20.43 ± 0.30	16	23	26	99	-18.40
482	-20.36 ± 0.25	66	24	73	-20.11 ± 0.27	77	20	85	98	-18.63
485	-20.17 ± 0.27	54	19	68	-20.10 ± 0.28	62	18	78	100	-18.73
495	-20.04 ± 0.15	95	40	97	-20.11 ± 0.13	97	45	99	100	-18.47
499	-19.57 ± 0.27	90	14	81	-19.68 ± 0.25	94	16	85	99	-18.45
519	-20.46 ± 0.26	93	22	96	-20.44 ± 0.25	95	23	96	100	-18.00
524	-18.96 ± 0.17	78	13	9	-19.09 ± 0.16	77	14	12	94	-18.35
553	-19.92 ± 0.25	93	15	93	-19.76 ± 0.27	99	13	96	100	-18.00
557	-19.57 ± 0.18	77	15	30	-19.47 ± 0.19	69	13	18	99	-18.00
575	-20.35 ± 0.23	43	20	14	-20.42 ± 0.20	32	23	7	100	-18.51
606	-21.26 ± 0.51	41	12	30	-21.13 ± 0.41	53	15	35	90	-18.00
653	-19.84 ± 0.33	100	10	96	-19.62 ± 0.26	97	10	77	97	-18.00
658	-19.27 ± 0.36	77	5	45	-19.16 ± 0.24	93	6	28	99	-18.00
683	-20.79 ± 0.25	51	42	46	-20.77 ± 0.23	58	43	52	100	-18.70
699	-19.89 ± 0.15	82	35	83	-19.90 ± 0.14	82	37	81	100	-18.21
712	-23.95 ± 1.00	63	10	50	-21.60 ± 0.68	52	12	46	99	-18.21
722	-20.32 ± 0.22	62	28	67	-20.48 ± 0.29	70	25	68	98	-18.00
726	-19.77 ± 0.21	70	15	52	-19.30 ± 0.30	82	10	43	88	-18.00
728	-20.22 ± 0.23	51	19	62	-19.98 ± 0.31	77	14	88	99	-18.00
735	-19.42 ± 0.18	79	12	17	-19.42 ± 0.16	88	13	8	99	-18.00
742	-19.57 ± 0.16	30	17	12	-19.40 ± 0.25	33	11	12	82	-18.00
748	-19.76 ± 0.30	61	10	68	-19.92 ± 0.21	42	12	28	10	-18.00

to the composite from the simulations. There are two exceptions to the corollary, however: both E438 and E462 have unexceptional probabilities from the two-sample χ^2 test, but are excluded at the 5 per cent level from the simulations.

If we include only those clusters where the derived M^* lies outside the 1 per cent confidence level from the simulations (as taken from Table 2) for one or other of the background subtraction methods, then only clusters E400, E429

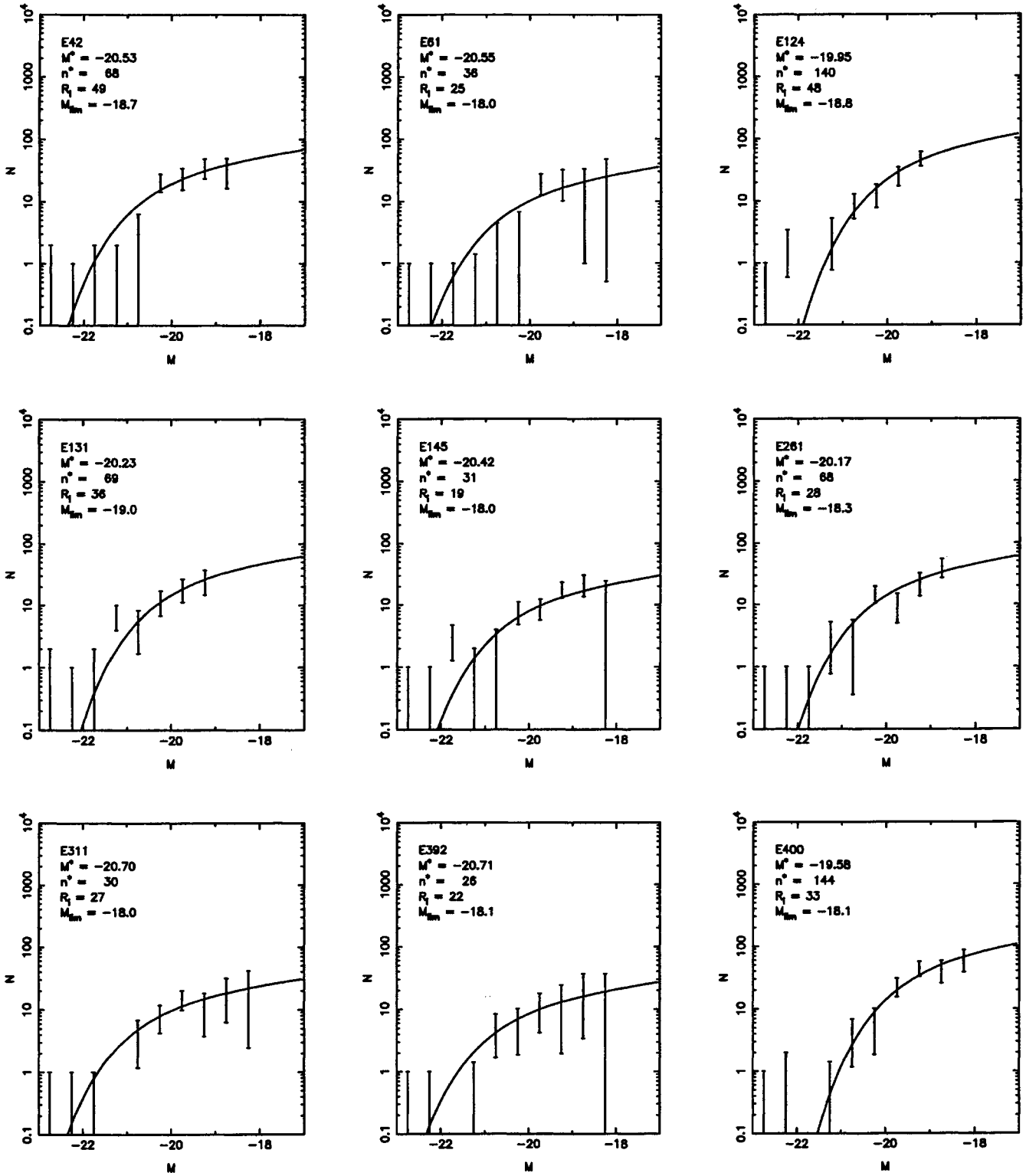

Figure 6. Measured luminosity functions for all those clusters with measured richness values, R_i, of 15 or more using the local background correction method. The best one-parameter fit to the Schechter function is shown by a solid line. The fit is over the range $-21 < M < M_{\rm lim}$.

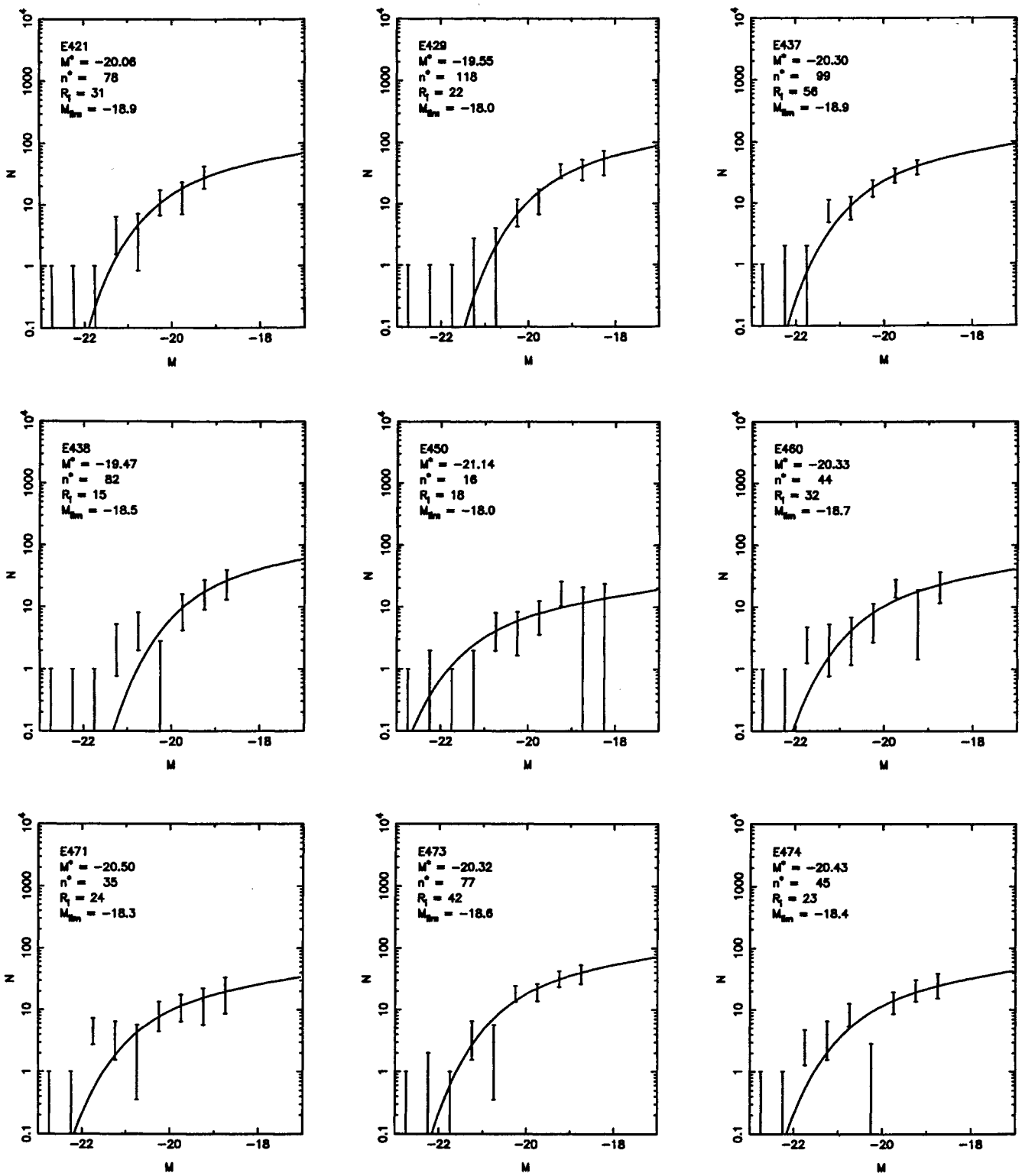

Figure 6 – *continued*

and E524 show strong evidence for an LF that differs from the composite. All three of these clusters also disagree at the 5 per cent level when considering both background subtraction methods. At the 5 per cent level, there are several additional clusters that disagree. Leaving aside those in which only one of the background subtraction methods gives divergent results (E499, E726), we are left with E438, E462 and E742. All of these, except E400 and E429, have a value of $R_i \leq 15$, so we may reasonably exclude these as being different on the grounds that accurate background subtraction is crucial for these clusters, and, as found in Section 4, errors of 0.5 mag in the fitted value of

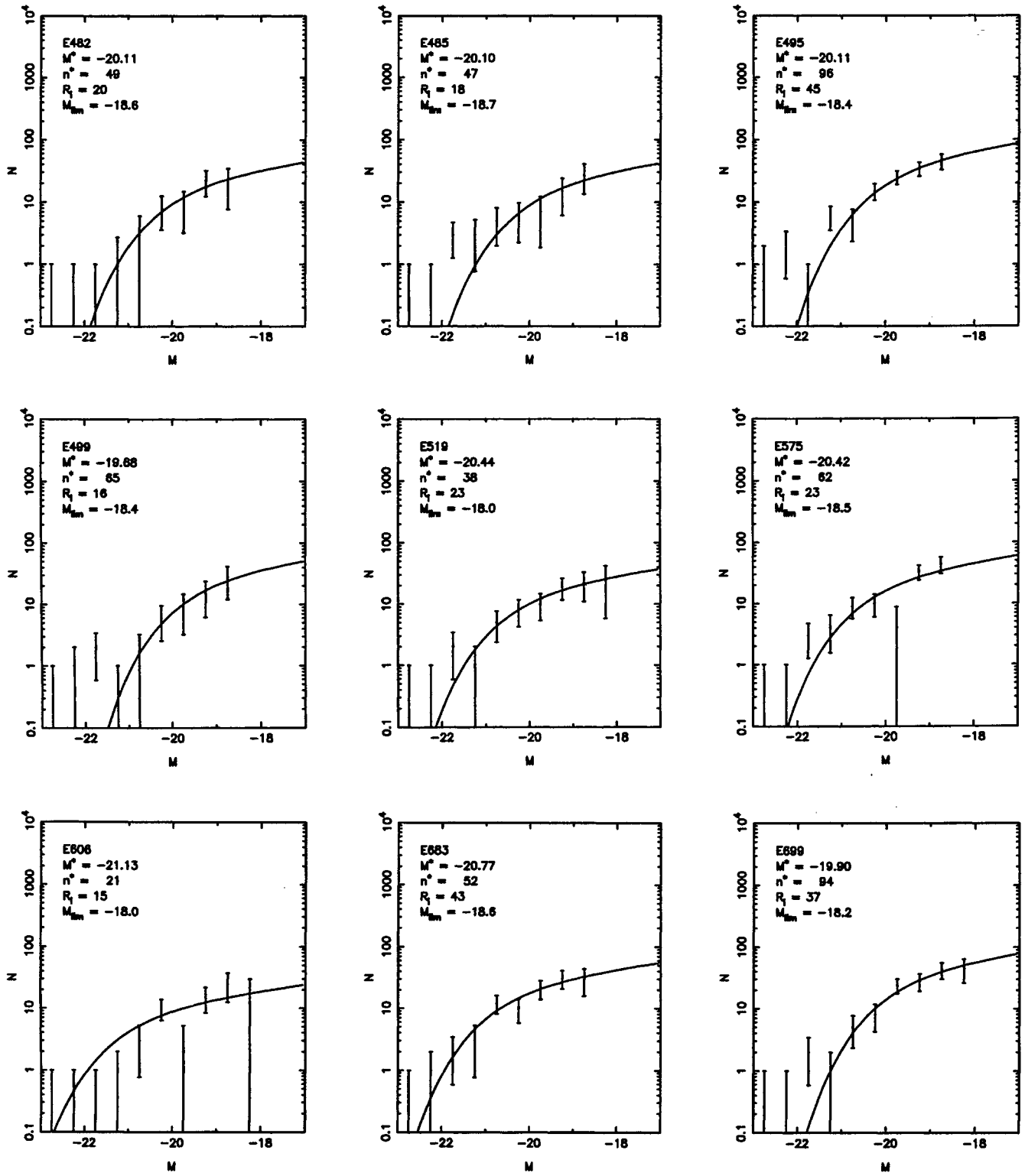

Figure 6 – *continued*

M^* are easily accounted for by an inappropriate background correction. This leaves only E400 and E429. It can be seen from Table 4 that even the direct χ^2 comparison of their LFs with the composite might lead to them being thought discrepant. The LFs of these clusters are apparently normal (see Fig. 6). However, before concluding that these clusters do show a significant difference, we first consider the possibility that there may be some problem with the data. Examination of the data in Collins et al. (1995) shows that all of these clusters have good reliable redshifts, with the positions of the galaxies for which redshifts were obtained agreeing well with the cluster centres given in

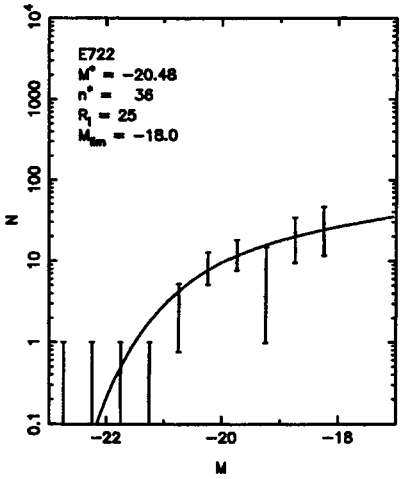

Figure 6 – *continued*

Table 1. Further, we note that for the cases of E400 and E429, other clusters appear on the same photographic plate and do not have discrepant M^*, hence the photometry of these systems should be good. Therefore, we find that there are at least two clusters that do not have the same LF as the derived composite. This is in keeping with earlier studies by Dressler (1978), Lugger (1986) and Colless (1989) who found that ~ 10 per cent of their clusters similarly did not agree with the mean Schechter LF they derived.

5.3 Dependence of the LF on cluster properties

The major advantage of our sample over previous studies is that it is large enough that we can test the dependence of the LF on intrinsic cluster properties. In particular, we will consider the possible variations with cluster richness (as defined by R_i), Bautz–Morgan (BM) class, which we have taken from the Abell, Corwin & Olowin (1989) catalogue, and velocity dispersion (taken from Collins et al. 1995).

For each case we split our total sample into two, and used the local background correction method only. When comparing different richness samples we used the cuts $10 < R_i < 20$ and $R_i > 20$ (which is of course just the composite LF derived previously). For BM class, we considered only those of type I and III, and counted intermediate types (e.g. type I–II) as type II which we did not use. In this way we sought to maximize the differences between the clusters to test for any effect on the LF. We split the sample into two in velocity dispersion using a cut at 700 km s^{-1}. Unfortunately, most of the very high-velocity dispersion clusters (those with $v > 1000$ km s^{-1}) are also the most distant, making it difficult to constrain α, and leaving few bins in the data with which to compare the two sets using a χ^2 test. We therefore were forced to use a lower-velocity cut-off for our high-velocity dispersion sample than Colless (1989) did, and so did not sample the same part of parameter space as he did.

Since we do not have well-defined velocity dispersions for all clusters, and those which are not in the Abell, Corwin & Olowin catalogue do not have BM classes, the two subsamples do not comprise all of the observed clusters. The number of clusters comprising each subsample is given in Table 5. In addition, for the velocity dispersion and BM samples we have included two richness cuts, at $R_i > 20$ and $R_i > 15$. This provides some indication of the stability of the result on the clusters making up the actual subsamples. We give both one- and two-parameter fits to the Schechter LF in Table 5. For the one-parameter fits we again used $\alpha = -1.25$. The results from this analysis are also shown in Fig. 7. We have also compared the LFs for these subsamples against the composite derived in Section 5.1, and against each other, using a two-sample χ^2 test, as well as comparing the subsamples directly with the results of our simulations (Fig. 4). The results of the two-sample χ^2 test are also given in Table 5. Since n^* can vary between these different sets of clusters, we rescaled the binned data before the comparison, so that the derived R_c values from the composites agreed.

There are noticeable differences between the richness cuts for both the BM class III clusters and the high-velocity dispersion clusters, with the richer subsamples having a notably poorer fit to the standard Schechter LF, and being discrepant compared to the composite. However, only one cluster contributes to the faintest bin in the richer subsample, and only one other is added to that when the poorer limit is considered. If we exclude this bin, then very similar fits are found for both richness limits and the discrepancy is removed. It is clear from this that variations in the LF due to the last bin alone are not significant. We do not consider these two subsamples further.

Once these discrepant sets are removed, it is clear that neither BM class shows any evidence for deviation from a universal LF, nor do they differ from each other, according to any of the tests applied. The same is true for the split according to richness alone, where the fits to both samples are very similar within the derived errors. The actual 'goodness' of the fit for the lowest richness sample is poor, but this most likely reflects difficulties in background correction at these low richness values as noted previously.

For the $R_i > 15$ velocity dispersion samples, there is weak evidence that the two samples differ from each other (significance ~ 54 per cent). When compared with the composite, neither sample shows any evidence for difference when using the two-sample χ^2 test. However, when compared with the Monte Carlo simulations, we find that the higher velocity dispersion clusters are clearly unlikely to have been drawn from the same basic distribution as the composite (at much better than the 1 per cent level). We therefore find that there may be evidence for some dependence of the LF on velocity dispersion.

It is worth considering the effect of including the brighter galaxies as well in this analysis. As is readily evident from Fig. 7, there is little difference between the rich and poor samples across the entire range of M, and the differences for the high- and low-velocity dispersion samples is largely restricted to the fainter galaxies. Considering the $R_i > 15$ BM samples, however, there are clearly fewer bright galaxies in ther BM class I sample than in the BM class III sample. This is not a normalization effect, since the two samples have essentially the same LFs at fainter magnitudes. Again, however, we caution against overinterpretation of this difference.

Lastly, we note that all of the velocity dispersion subsets, and the low-richness subset, can formally be excluded as

Table 5. Fits to the subsets of the full cluster data as described in the text. The columns are: the description of the subset; the derived values of M^* and α (again, the error corresponds to the values of M^* and α where $\chi^2 = \chi^2_{\rm min} + 1$); the formal likelihood that the fit is good; the number of clusters that have been combined to form the composite for the subset; the derived value of n^*; the measured value of the cluster richness; and lastly, the probability that the subset and the composite derived in Section 4.1 have the same distribution using a two-sample χ^2 test. The first row for each entry gives the best two-parameter fit, the second gives a one-parameter fit with $\alpha = -1.25$. Those entries that appear only in the first row have the same values in the second.

Sample	M^*	α	p(fit)	n_{clus}	$n_{clus}n^*$	R_c	p(CLF)
BM class I ($R_i > 20$)	-20.44 ± 0.14	-1.28 ± 0.04	69	8	400	260	> 99
	-20.37 ± 0.08	-1.25	83		430		
BM class I ($R_i > 15$)	-20.35 ± 0.14	-1.24 ± 0.05	63	9	480	280	> 99
	-20.37 ± 0.08	-1.25	78		470		
BM class III ($R_i > 20$)	-22.60 ± 5.80	-2.00 ± 0.03	79	8	21	250	16
	-19.82 ± 0.10	-1.25	12		860		
BM class III ($R_i > 15$)	-20.56 ± 0.18	-1.49 ± 0.04	74	10	360	280	> 99
	-20.09 ± 0.07	-1.25	77		670		
$v < 700 \mathrm{kms}^{-1}$ ($R_i > 20$)	-20.01 ± 0.01	-0.93 ± 0.01	96	18	1470	600	96
	-20.56 ± 0.07	-1.25	66		800		
$v < 700 \mathrm{kms}^{-1}$ ($R_i > 15$)	-19.98 ± 0.04	-0.92 ± 0.03	69	22	1700	660	88
	-20.56 ± 0.08	-1.25	46		900		
$v > 700 \mathrm{kms}^{-1}$ ($R_i > 20$)	-20.31 ± 0.02	-1.66 ± 0.01	98	6	320	200	13
	-19.66 ± 0.07	-1.25	72		840		
$v > 700 \mathrm{kms}^{-1}$ ($R_i > 15$)	-19.79 ± 0.02	-1.20 ± 0.02	88	7	730	220	88
	-19.87 ± 0.06	-1.25	95		660		
$10 \leq R_i < 20$	-19.86 ± 0.27	-1.25 ± 0.15	7	15	700	220	69
	-19.86 ± 0.07	-1.25	13		700		

being drawn from a model of the composite LF with α fixed at -1.25 on the basis of the one-parameter fits. Small deviations in both M^* and α mean that the one-parameter fits are distinct from the composite derived in Section 5.1. It is clearly dangerous to compare such subsamples (with their relatively small intrinsic errors) using such methods.

6 DISCUSSION

6.1 Comparison with previous results

First, we compare our derived estimates for the composite LF, for all clusters with $R_i > 20$, with those derived previously. Colless (1989) gives the best fits from previous data in his table 2, scaled into the colour and value of H_0 that we are using. Excluding Colless' own data, this shows that the quoted values of M^* and α are -19.9 and -1.24 respectively, with typical errors in M^* of 0.5, when the brightest cluster galaxies are excluded from the fit. Colless himself finds $M^* = -20.04$ and $\alpha = -1.21$ for a two-parameter fit similar to ours. These values are in good agreement, within the errors, with those derived by us. It is clear that the luminosity functions of moderately rich clusters, when considered across this relatively narrow range in absolute magnitude, are indeed very similar on average.

In addition we can compare our one-parameter fits for three clusters with those given by Colless (1989). EDCC clusters 394, 400 and 124 correspond to his clusters C02, C03 and C52. From Table 4 we can see that when a comparison is made of similar fitting procedures (i.e., χ^2 fitting and using a global background correction), the agreement is excellent. Colless quotes values for M^* of -19.76 ± 0.21, -19.86 ± 0.23 and -20.05 ± 0.33 for C02, C03 and C52 respectively. Although the original photographic plates used in both studies are the same, a different measuring machine was used (the APM), with consequent differences in the reduction from measuring machine magnitudes to final derived astronomical magnitudes. Therefore, this agreement for the specific clusters that are common to the two studies is highly encouraging. It is worth making some specific comments on these clusters, however. E394 was found by Colless to be discrepant with both the fit by a Schechter LF and with a comparison with his composite LF. We note that Table 4 shows that whilst the global background correction gives a moderate probability for both the fit and the comparison with the composite, the local background correction method gives better agreement. This difference shows in the direct comparison of the magnitude distributions for the two background correction methods (Table 4). This is clearly an example in which global background correction gives rise to these deviations. We note that E394 is one of the poorest clusters in both our sample and that of Colless. Colless found tht E124 was marginally discrepant when compared against the composite LF. We find no evidence for any difference. Lastly, E400, which we found in Section 5.2 to be potentially significantly different

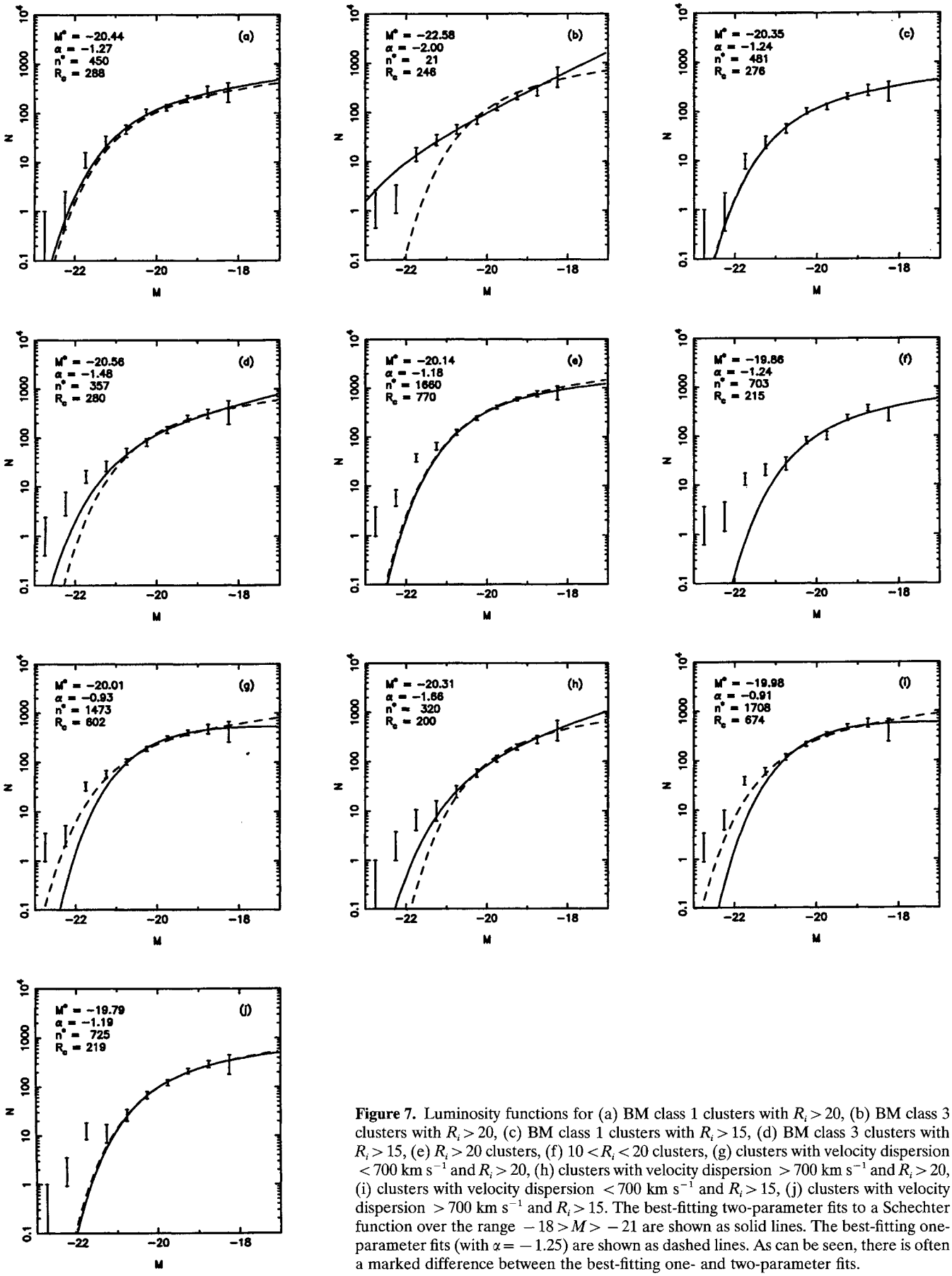

Figure 7. Luminosity functions for (a) BM class 1 clusters with $R_i > 20$, (b) BM class 3 clusters with $R_i > 20$, (c) BM class 1 clusters with $R_i > 15$, (d) BM class 3 clusters with $R_i > 15$, (e) $R_i > 20$ clusters, (f) $10 < R_i < 20$ clusters, (g) clusters with velocity dispersion < 700 km s^{-1} and $R_i > 20$, (h) clusters with velocity dispersion > 700 km s^{-1} and $R_i > 20$, (i) clusters with velocity dispersion < 700 km s^{-1} and $R_i > 15$, (j) clusters with velocity dispersion > 700 km s^{-1} and $R_i > 15$. The best-fitting two-parameter fits to a Schechter function over the range $-18 > M > -21$ are shown as solid lines. The best-fitting one-parameter fits (with $\alpha = -1.25$) are shown as dashed lines. As can be seen, there is often a marked difference between the best-fitting one- and two-parameter fits.

from the composite, Colless finds to be a reasonable match. However, since this cluster gives a difference for both background subtraction methods, we find our result to be reliable. We also note that the smaller errors derived for by us for both E400 and E124 allow us to make more definitive statements than Colless can for these clusters.

Finally we note that, unlike Colless, we find that all the subsets of the data we took are well-fitted by a one-parameter Schechter LF, though they are not necessarily in agreement with the fit to the composite.

6.2 Implications for cluster formation models

There have been few detailed N-body simulations of the formation of clusters that have suitable dynamic range to map out the whole of the expected LF as a function of the cosmological model assumed. For example, van Kampen (1995) makes simple predictions for the LF based on extensive simulations, but is led to the conclusion that this modelling cannot correctly account for all of the merging that takes place within the cluster. His fit to the bright end of the luminosity function (which we might expect to be easier to model) is similar to the one observed.

There have been studies that lead to simpler predictions as to the expected form of the LF according to the dominant processes that occur during cluster formation. The mode of cannibalism for the growth of cD galaxies as suggested by Hausman & Ostriker (1978) predicts that there should be differences between the luminosity function when broken down by BM class. We see no real evidence for such a difference when we consider the range $-18 > M > -21$. There is an indication for such a trend in the galaxies brighter than $M = -21$, in the sense that the BM class I sample has fewer bright galaxies. However, better photometry of the bright galaxies would be required to confirm this result. Merritt (1983, 1984) argued that most of the properties of clusters are essentially 'frozen in' when they form and that merging and tidal stripping processes are ineffective in rich cluser cores. This leads to the prediction that the LF should appear to be much the same from cluster to cluster. However, *Hubble Space Telescope* imaging data of moderate redshift clusters (e.g. Dressler et al. 1994) tends to rule against such a model, since it provides convincing evidence that mergers are important at least in the early stages of cluster evolution. One possibility is that the bulk of the change in the LF between clusters occurs only amongst the very faintest or brightest galaxies, the regime to which our data is insensitive. For example, it is known that some clusters show an upturn in the LF at faint magnitudes (e.g. Driver et al. 1994, Bernstein et al. 1995), and there has always been marginal evidence for greater deviations in the LF when the brightest cluster galaxies are included (e.g. Lugger 1986 and the comments in Section 5.1), though we again caution against over-interpretaton of results on the brightest cluster members. However, our data clearly shows that in the region of the 'break' in the LF, the cluster-to-cluster variance is extremely small.

7 CONCLUSIONS

We have considered the cluster galaxy luminosity function as derived from data in the Edinburgh–Durham Southern Galaxy Catalogue and the Edinburgh–Milano Redshift Survey. Our data set is the largest multi-redshift cluster sample to be considered to date for this purpose. From this we find the following.

(i) Our data shows that there is strong evidence that *most* clusters have very similar LFs when both the brightest and faintest galaxies are discarded. The average of the composite LFs derived using the three-background correction methods in Section 5.1 give $M^* = -20.16 \pm 0.02$ and $\alpha = -1.22 \pm 0.04$, when the LF is determined in the range $-18 > M > -21$.

(ii) We find a very good agreement between our results and those derived by Colless (1989) from similar input data, and with the mean of the data presented by Dressler (1978) and Lugger (1986).

(iii) We have tested the stability of the derived Schechter luminosity function parameters to the type of background correction made. We find excellent agreement between a method based on a global background correction and that based on a strictly local correction. However, the largest sysematic error remaining in our derivation of the best-fitting parameters for the composite LFs is the background correction, with an uncertainty of up to 0.05 in M^* and 0.05 in α possible.

(iv) We also tested the universality of the luminosity function, by comparing individual cluster LFs with the composite function derived in Section 5.1, and by testing each cluster LF separately against a Schechter function (Section 5.2). From this we find that at most ~ 10 per cent of the clusters may have LFs that are significantly different from the composite.

(v) We also broke our sample into sub-samples defined by richness, BM class and velocity dispersion (Section 5.3). From these tests we found weak evidence that the high- and low-velocity dispersion samples have different composite LFs, and that the higher velocity dispersion clusters may have a different LF from the global composite. This agrees with the marginal detection of a difference between similar samples by Colless (1989). We also found evidence for differences between the BM class samples, but only for the brightest galaxies ($M < -21$) that we otherwise excluded for reasons of photometric reliability (Section 3.4). The evident trend is in line with the predictions of the cannibalism model of Hausman & Ostriker (1978), but we caution against over-interpretation of this result without more reliable photometry for the bright galaxies. There is no evidence for any convincing difference between the other subsets of the data. Our results and our simulations do, however, show that it is important to consider more than one method of testing the differences between subsets of the data. On the basis of a one-parameter fit alone we have concluded that there were significant differences between the low- and high-velocity dispersion samples and the composite, and between the low- and high-richness clusters. The other tests show no evidence for any difference, however, with the exception of the high-velocity dispersion clusters where the two-parameter fits and Monte Carlo simulations show weak evidence for a difference from the composite.

It is likely that to make any further progress on the nature of the cluster galaxy luminosity function we will need to overcome the limitations of data such as ours. First, there is

clearly a need to derive cluster membership free of any correction for backgrounds, by obtaining sufficient redshifts to allow us to actually map the galaxy distribution in three dimensions around the cluster. Secondly, better photometry is required to tie down the bright and faint ends of the LF. Given these, it should be possible not only to discriminate between differences in the data broken down by richness, velocity dispersion or whatever else is desired, but also to test for the differences that our data suggest may exist in the LF when comparing the very brightest and very faintest galaxies.

ACKNOWLEDGMENTS

SLL would like to acknowledge the support of an SERC Post-doctoral Fellowship during the early part of his work on the EDCC. CAC acknowledges the support of PPARC through an Advanced Fellowship. We would like to thank the referee, Steve Maddox, for his comments.

REFERENCES

Abell G. O., 1975, in Sandage A., Sandage M., Kristian J., eds, Stars and Stellar Systems IX: Galaxies and the Universe. Univ. Chicago Press, Chicago, p. 601
Abell G. O., Corwin H. G., Olowin R. P., 1989, ApJS, 70, 1
Bernstein G. M., Nichol R. C., Tyson J. A., Ulmer M. P., Wittman D., 1995, AJ, 110, 1507
Colless M., 1989, MNRAS, 2137, 799
Collins C. A., Nichol R. C., Lumsden S. L., 1992, MNRAS, 254, 295
Collins C. A., Guzzo L., Nichol R. C., Lumsden S. L., 1995, MNRAS, 274, 1071
Dressler A., 1978, ApJ, 223, 765
Dressler A., Oemler A., Sparks W. B., Lucas R. A., 1994, ApJ, 435, L23
Driver S. P., Phillips S. P., Davies J. I., Morgan I., Disney M. J., 1994, MNRAS, 268, 393
Ellis R. S., 1983, in Jones B. J. T., Jones J. E., eds, The Origin and Evolution of Galaxies. Reidel, Dordrecht, p. 225
Geller M. J., Beers T. C., 1982, PASP, 94, 421
Guzzo L., Collins C. A., Nichol R. C., Lumsden S. L., 1992, ApJ, 393, L5
Hausman M. A., Ostriker J. P., 1978, ApJ, 224, 320
Heydon-Dumbleton N. H., 1989, PhD thesis, Univ. Edinburgh
Heydon-Dumbleton N. H., Collins C. A., MacGillivray H. T., 1989, MNRAS, 238, 379
Lugger P., 1986, ApJ, 303, 535
Lumsden S. L., Nichol R. C., Collins C. A., Guzzo L., 1992, MNRAS, 258, 1
Maddox S. J., Sutherland W. J., Efstathiou G. P., Loveday J., Peterson B. A., 1990, MNRAS, 247, 1
Malumuth E., Richstone D. O., 1984, ApJ, 276, 413
Merritt D., 1983, ApJ, 264, 24
Merritt D., 1984, ApJ, 276, 26
Merritt D., 1985, ApJ, 289, 19
Metcalfe N., Shanks T., Fong R., Jones L. R., 1991, MNRAS, 249, 498
Nichol R. C., Collins C. A., 1993, MNRAS, 265, 867
Nichol R. C., Collins C. A., Guzzo L., Lumsden S. L., 1992, MNRAS, 255, 21P
Richstone D. O., 1975, ApJ, 200, 535
Richstone D. O., 1976, ApJ, 204, 642
Schechter P. L., 1976, ApJ, 203, 297
van Kampen E., 1995, MNRAS, 273, 295